

Solvent effects as probes of the dynamical factors controlling sub-nanosecond photoprocesses: the case of $W(CO)_5$ pyridine

Cooper H. Langford *, Lawton E. Shaw

*A101, The University of Calgary 2500 University Drive NW, Calgary,
Alberta. T2N 1N4, Canada*

Received 22 December 1995

Contents

Abstract	221
1. Introduction	222
2. Theoretical considerations	224
2.1. Overview	224
2.2. Solvent effects	224
2.3. Pressure effects	226
3. Experimental aspects of the reactions of $W(CO)_5L$	227
4. Solvent effects on reaction of $W(CO)_5L$	228
5. Interpretation	231
Acknowledgements	232
References	232

Abstract

Quantum yields for the formation of $W(CO)_5S$ (S =solvent) from $W(CO)_5L$ (L =pyridine, other bases) are solvent and wavelength dependent. The reactions are determined by processes occurring in the femtosecond to short picosecond time domain in competition with vibrational relaxation. Tools are needed to probe the dynamical events in this short time domain. The aim would be the detail of mechanistic analysis that is achieved in study of the slower reactions from vibrationally equilibrated excited states using structure–reactivity correlation and transition state theory. In this review, the case study of $W(CO)_5$ pyridine is used to suggest ways to use solvent effects and pressure dependence for understanding of dynamic processes. Special attention is given to two ‘solvent cage effects’: the classic cage effect related to viscosity and the recently recognized thermal cage effect related to solvent bulk thermal conductivity. The special utility of dynamical parameters of the bulk solvent as aids in analysis of fast dynamics

* Corresponding author. E-mail: chlangfo@acs.ucalgary.ca.

in photochemistry is emphasized. The potential utility of molecular dynamic simulation is explored. © 1997 Elsevier Science S.A.

Keywords: Cage effect; Sub-nanosecond photoprocesses

1. Introduction

In the last few years, femtosecond time resolution has become directly available. The results have been of fundamental importance. They indicate that quantum yields of many photoreactions are determined in times of the order of 100 fs. This is close to the period of vibration of a metal–ligand bond with a stretching frequency of 350 cm^{-1} . The best characterized case in transition metal complex photochemistry is that of CO dissociation from $\text{M}(\text{CO})_6$ [1] where $\text{M} = \text{Cr}, \text{Mo}, \text{or W}$. In each of these cases the overall quantum yield for photosubstitution is less than one and some competing pathways for the fate of excited states or early intermediates must be involved. In the specific case of $\text{W}(\text{CO})_6$ in hexane, for example, formation of the vibrationally relaxed primary product, $\text{W}(\text{CO})_5\text{S}$ ($\text{S} = \text{solvent}$) is completed with a time constant of 17 ps [1,2], where the primary dissociation is complete within 300 fs. It is clear that factors determining the overall quantum yield depended upon initial events in a domain too fast for the Born–Oppenheimer approximation and that subsequent behaviour of the reactive primary intermediates will defy the quasi-equilibrium assumption of transition state theory — namely, that all but one coordinate is at a Boltzmann equilibrium.

As with thermal kinetics, assignment of mechanistic pathways in photochemistry depends upon studies of variation of reactivity with structure and the role of solvent, temperature, and pressure. These variables have been successfully interpreted using transition state theory concepts such as ‘apparent activation energies’ and ‘apparent volumes of activation’ when photochemistry involves excited states of sufficient lifetime for reaction to arise from vibrationally equilibrated excited states. In the case that reaction pathways are determined in times short compared with vibrational equilibration (i.e. tens to hundreds of picoseconds) we need to find new ways to understand dependence on solvent, temperature, and pressure. It is the purpose of this paper to explore some of the possibilities that are open and to describe studies of the system $\text{W}(\text{CO})_5\text{L}$ ($\text{L} = \text{pyridine (py)}, \text{piperidine (pip)}$) which provides preliminary indication of the application of these possibilities.

A word on the choice of the $\text{W}(\text{CO})_5\text{L}$ system. $\text{W}(\text{CO})_6$ appeared at one time to be a classic example for assignment of a long-lived reactive excited state, the quantum yield is wavelength independent over a wide range and triplet sensitizers produce an equivalent quantum yield [3]. This would appear to imply efficient crossing from higher states to the lowest triplet and a quantum yield determined by the fate of the nanosecond lifetime triplet. The femtosecond results show that the evidence is misleading in this respect. In the case of $\text{W}(\text{CO})_5\text{L}$, quantum yields are richly wavelength- and medium-dependent [4,5]. That the reaction is similarly fast is demonstrated by a picosecond study that shows that vibrationally relaxed

$\text{W(CO)}_5\text{S}$ is formed in less than 10 ps from $\text{W(CO)}_5\text{py}$ (compared with 17 ps for W(CO)_6) [4]. The reason for faster $\text{W(CO)}_5\text{S}$ vibrational relaxation in the case of py dissociation is probably that the polyatomic py ligand can carry off a much larger share of the vibrational excess energy than the stiff diatomic ligand, CO. Additional support for the rapidity of processes in $\text{W(CO)}_5\text{L}$ comes from cases where L is a ligand with a vacant $\pi^*\text{MO}$. In this case, sub-picosecond intersystem crossing to a $^3\text{MLCT}$ state has been observed [6].

Fig. 1 shows that reactions of $\text{W(CO)}_5\text{L}$ are clean and convenient to monitor by absorption spectroscopy. Table 1 summarizes the wavelength dependence for the reaction of $\text{W(CO)}_5\text{L}$ with 1-hexene in iso-octane. The role of the 1-hexene is simply to capture the solvo intermediate, $\text{W(CO)}_5\text{iso-octane}$, to form a stable product. A striking observation is that the yields on irradiation into the singlet region (313 to 436 nm) are higher than those for irradiation into the triplet region (488 nm). Careful

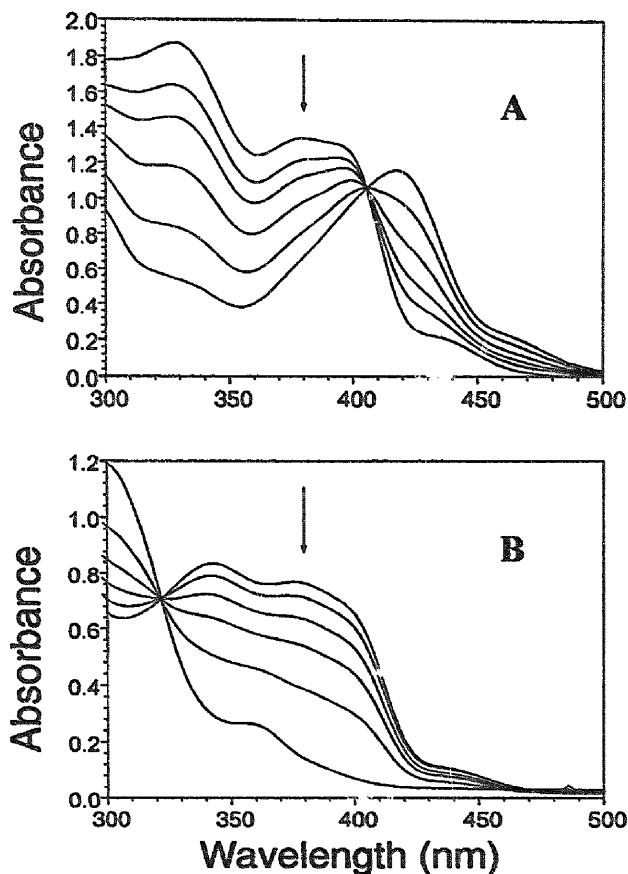


Fig. 1. Spectral changes during photolysis of $\text{W(CO)}_5\text{py}$ in (A) methanol and (B) 24:1 chloroform–1-hexene.

Table 1

Photosubstitution quantum yields for $W(CO)_5L \rightarrow W(CO)_5(1\text{-hexene})$ in the solvent system iso-octane–1-hexene (2:1)^a

L		Quantum yields				
		313 nm ^b	365 nm ^b	436 nm ^b	457.9 nm ^b	488.0 nm ^b
Pyridine	N ₂	0.48(0.02) ³	0.54(0.02) ¹³	0.63(0.04) ¹⁰	0.42 (0.04) ¹³	0.23(0.02) ¹⁴
	O ₂	0.52(0.03) ⁴	0.55(0.03) ¹²	0.64(0.06) ⁵	0.44 (0.03) ⁷	0.22(0.01) ⁴
Piperidine	N ₂		0.48(0.03) ¹¹	0.53(0.02) ⁶	0.42 (0.02) ⁴	0.38(0.02) ⁴
	O ₂	0.47(0.02) ³	0.51(0.02) ⁵	0.51(0.02) ⁵	0.44 (0.01) ⁶	0.38(0.02) ⁵

^a Concentrations of reactants are between 1.5×10^{-4} and 6.5×10^{-4} M. Light intensities are between 3×10^{-10} and 2×10^{-6} einstein s⁻¹. Numbers in parentheses represent standard deviations. Superscripts represent the numbers of trials. ^b Wavelengths are ± 2 nm.

analysis of primary products in solvents where the solvent has more than one atom that may initially coordinate to the W atom suggests that the stereochemistry of the process may differ between the singlet and triplet regions [7]. The behaviour of the system is sufficiently complex to make it a good test system for the effects of the diagnostic variables.

2. Theoretical considerations

2.1. Overview

The best studied of fast reactions in solution is probably the dissociation and recombination of I₂. The great advantage is the wealth of detailed spectroscopic information accessible. A fairly precise map has been drawn of the events leading to the recombination or irreversible dissociation of a pair of I atoms created by excitation of I₂. On the basis of this work, Harris et al. [8] have proposed a generalized picture of events to be considered in the short time domain of species at high energy (see Fig. 2). It includes cage escape to yield products A, primary recombination via relaxation to the ground state C, and trapping in local high energy excited state potential minima B. We wish to diagnose the competition among these processes.

2.2. Solvent effects

Solvent effects are a particularly valuable tool for analysis of fast processes. This is because bulk solvent parameters can be used to help to distinguish four types of dynamic process which may determine the sequence of fast events.

(1) The cage effect is well known in its mechanical manifestation. The presence of surrounding solvent molecules can cause escaping geminate partners to rebound, favouring recombination over escape. It has long been recognized that this cage

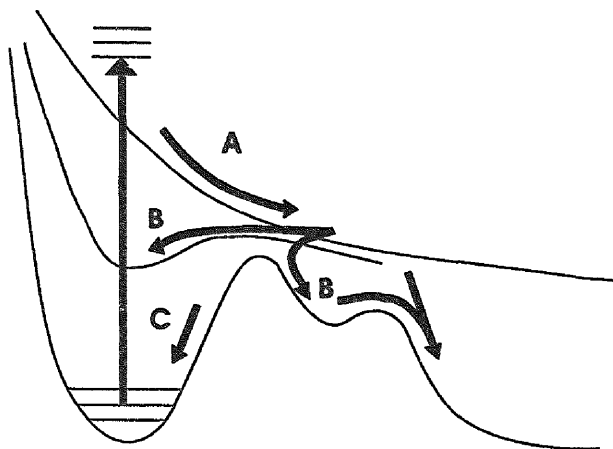


Fig. 2. Harris et al. [9] suggest a conceptual two-dimensional diagram as the way to think about competing pathways in the short time domain. **A** represents prompt dissociation of a bond. **B** denotes trapping. **C** denotes vibrational relaxation back to the ground state. The 10–100 ps time scale of process **C** defines the outer limits of the time scales for competition among processes **A** and **B** which provide for multiple pathways such as are observed in the case of $W(\text{CO})_5\text{L}$.

effect decreases with increasing solvent fluidity ($1/\eta - 1/\text{bulk viscosity}$). Since cages have nanosecond lifetimes at room temperature, it is likely that large excess energies are needed to support escape from the cage in picosecond times [10].

(2) In addition to the mechanical cage effect, there is a thermal cage effect which has only been recognized recently [11]. As excess vibrational and librational energy is transferred from an initially excited molecule to its surrounding solvent cage, these molecules become 'hotter'. Their propensity to accept further energy is reduced until they are able to dissipate that energy further out into the surroundings. The 'thermal cage' was first recognized from studies of vibrationally excited ground states and lowest singlets of large organic dye molecules. The low frequency tail of the absorption spectrum and the high frequency tail of the emission spectrum act as molecular thermometers and evolution of the spectral envelope monitors the time scale of cooling. For excess energies of up to $15\,000\text{ cm}^{-1}$ in azulene, cooling time constants range from 8 ps in ethanol to 30 ps in acetonitrile. Theoretical models of energy transfer cooling of hot azulene in the dilute gas phase are good. Extrapolation of the energy loss rates to the liquid phase by increasing collision frequencies gives values much too high compared with the experiments. The discrepancy is removed by a two stage model.

Vibrational and translational energy is transferred from the hot solute to the neighbouring solvent shell by collisions in the first stage. The dissipation of energy within the solvent is approximated by the macroscopic theory of heat conduction. The hot solute interacts with an essentially fixed cage of solvent neighbours (cage effect). The dissipation process is well modelled using classical thermal conductivity theory and the thermal cage effect is closely linked to the bulk thermal conductivity

of the solvent θ . The thermal cage effect becomes more prominent as the thermal conductivity decreases. The correlation of organic dye relaxation with bulk thermal conductivity was good [11]. Times were in the picosecond domain (10–100 ps).

(3) Solvent reorientation is an important process in relaxation of an excited system. Recent studies have demonstrated that this has important femtosecond components [12]. Dielectric relaxation (requiring solvent dipole reorientation by rotation) controlled by the longitudinal dielectric relaxation time τ is found in the longer time domain. The time τ is also a measurable bulk parameter which has successfully explained variations of proton transfer rates among organic acids.

(4) Solvent friction is an effect associated with the exchange of energy among degrees of freedom of a dynamic system near the transition state and the surrounding medium. It is called friction because it can impede passage toward products along a reaction coordinate. It has also been suggested to depend upon the factors which control bulk solvent viscosity η .

Correlation of photochemical behaviour with the bulk solvent parameters $1/\eta$, θ , and τ , should help considerably in recognizing mechanical cage escape, trapping processes often associated with the rate of vibrational relaxation, and trapping processes dependent upon solvent dielectric relaxation. It may, finally, be reasonable to suggest that a reaction with little solvent dependence is determined by electronic factors.

2.3. Pressure effects

In 1989, van Eldik and coworkers reported that high pressure reduces the quantum yield for photosubstitution of py and several 4-substituted complex of the form $W(CO)_5py-X$ [9]. They calculated conventional transition state theory volumes of activation of 3 to 6 cm³ mol⁻¹. Now that we realize that the quantum yields are controlled by events in the femtosecond to short picosecond time scale, prior to vibrational relaxation, we need to seek a new approach to interpretation of the effect of pressure. In thermal kinetics where transition state theory is useful, volumes of activation have proved to be very helpful in diagnosis of mechanism. There is reason to be optimistic that pressure dependence studies will be similarly useful in study of very fast photoprocesses. The basis for this optimism is the recent molecular dynamics simulation study of the conformational interconversion of chair and boat cyclohexane [12]. Theoretical studies show that solvent has little effect on the potential energy surface for this reaction. The effect of pressure on this reaction is seen mainly in the time for formation of the solvent cage. The main processes occur in the femtosecond domain (although processes related to dipole reorientation can last into the picosecond domain).

The central issue in the molecular dynamics simulations is to evaluate the distribution of trajectories of the system near the transition state which include recrossing compared with those which proceed directly across the transition state toward product. If too much energy remains in the reaction coordinate for too long, the molecule may recross the transition state and fail to complete the reaction. The

reaction of boat–chair interconversion may be expressed in terms of a relatively simple coordinate system focusing on two angles: the hindered rotation coordinate and a generalized secondary rotation coordinate ψ which takes the molecule from one degenerate chair or boat conformation to another. Both of these angles depend on the position of all six C atoms of cyclohexane.

A solvent cage formed around the cyclohexane transition state will initially cause the solvent to do negative work on the reaction coordinate and hence cause energy transfer from the solute to the solvent at early times. However, a cage does not always form around a solute near its transition state. We see, in this case, recrossing trajectories where the work landscape shows no evidence of cage formation at early times. The restoring forces from the cage are not strong enough to deter motion away from the unstable intramolecular barrier. The cage does, however, allow the solvent to cool the molecule and aid its stabilization. The mechanism for the pressure acceleration of the rate is then clear. Pressure increase will surely enhance the formation of solvent cages in the 0.1 ps domain and diminish the number of recrossing trajectories via increased work on the molecule.

The extrapolation from cyclohexane to $W(CO)_5L$ is great. However, the issue in the $W(CO)_5L$ case is that of the irreversible dissociation of L. It is not unreasonable to suggest that the formation of solvent cages at early times is favourable to rapid dissipation of the excess excitation energy (cooling). Increasing pressure is expected to favour early formation of solvent cages. For the comparison, it is important to note that the wavelength used in the pressure experiments of Ref. [9] was 436 nm. Solvent effects (see below) suggest that ‘cooling’ favours the direct reaction but that a trap state exists which provides a competing pathway. We need information on the dynamics of the competition between direct reaction and trapping. Detailed simulation efforts will be necessary for the interpretation of pressure dependence of fast processes. Since resonance Raman spectroscopy has suggested a vibrational coordinate to use in a simple model of the reaction coordinate [1] (an asymmetric stretch vibration described as a ‘buckle’ mode [4]), and solvents with simple structure and little specific solute–solvent interaction are appropriate for these reactions, there is a real opportunity to obtain a view of the dynamics of the dissociation of py similar to that of the boat–chair interconversion.

3. Experimental aspects of the reactions of $W(CO)_5L$

It is now useful to describe some of the experimental aspects of the photochemical reactions. Table 2 shows the assignment of the spectra of $W(CO)_5py$ and $W(CO)_5pip$ achieved by deconvolution of the absorption envelopes [5]. The key wavelengths in photochemical studies are 313, 436, 458, and 488 nm. Irradiation at 488 nm excites the ligand field $^1A_1 \rightarrow ^3E$ transition (C_4 , symmetry). At 458 nm irradiation is still past the maximum of the triplet at 448 nm but in a region where the weak triplet band overlaps the tail of the stronger singlet. Irradiation at 436 nm excites the $^1A_1 \rightarrow ^1E$ ligand field transition which has been argued to be the transition which is most vibronically favourable for the dissociation of L according to

Table 2

Band maxima for transitions in $\text{W}(\text{CO})_5\text{L}$ determined from deconvolution of spectral bands

Solvent ^a	Band maxima (± 2 nm)						
	W→py CT	W(CO) ₅ py			W(CO) ₅ pip		
		¹ A	¹ E	³ E	¹ A	¹ E	³ E
Iso-octane	352	388	404	448	388	410	448
Iso-octane–1-hexene	352	388	404	448	388	410	448
1-Hexene	354	388	404	448	388	409	448
CCl ₄ –1-hexene	354	386	405	448	388	409	448
C ₆ H ₆ –1-hexene	344	382	402	446	385	408	440
CHCl ₃ –1-hexene	336	384	404	440	389	407	448
CH ₂ Cl ₂ –1-hexene	336	380	400	440	386	406	444

^a Mixed solvents are in 2:1 ratio with 1-hexene.

Hollebone's rules [4]. This transition is the lower component of the first spin allowed and Laporte forbidden transition with the orbital label $d\pi \rightarrow d_{\sigma^*}$, which has a ¹T₂ label in octahedral symmetry and populates a metal–ligand antibonding orbital. The upper ¹A₁ component in C_{4v} symmetry of this same transition in octahedral symmetry is populated by irradiation at 365 nm. In the case of py, there is also metal to ligand charge transfer character at this wavelength. At 313 nm components of the transition labelled ¹T₁ in octahedral symmetry are excited. The C_{4v} components of this band have not been definitively resolved. The transition has the same basic orbital character as the ¹T₂ transition.

The reactions are extraordinarily clean in all cases. Fig. 1 shows spectral changes for conversion of W(CO)₅py to W(CO)₅(1-hexene) in octane [13]. The excellent isosbestic point is characteristic of all of the reactions under discussion in this review. Typically, quantum yields are obtained from the 0 to 10% conversion region and are free of complications from secondary photolysis and inner filter effects. The complexes are also thermally non-labile and there is no correction for thermal reaction. Only at long irradiation times have occasional observations of white precipitates indicated some complication. This appears to arise from the catalysis of polymerization of olefins by the reactive system; removal of the precipitate restored the isosbestic point [5].

4. Solvent effects on reactions of W(CO)₅L

The first attempt to understand the solvent effects on these reactions was presented in 1991 [5]. It sought explanation from correlation with the conventional static solvent parameters which have been used successfully in many analyses based on transition state theory. Such parameters include: dielectric constant, which relates to charge redistribution in the transition state; the alternative of spectroscopic solvent polarity measures such as the *E*_T parameter; and the Gutmann acceptor number *AN*

which relates to solvent acidity. None of these proved helpful. It was recognized that dynamic parameters would be required; however, the factors outlined in the theoretical section of this paper were not yet clear, and the way to approach the organization of tests of dynamic parameters was not clear. It is interesting (compare below) that the only conclusion that the first attempt could reach was that vibrational energy transfer was a crucial factor.

In the light of the theoretical considerations, we can now frame the questions more precisely. If charge redistribution is not central, there remain two key bulk solvent parameters, fluidity $1/\eta$ and thermal conductivity θ . A well designed experimental study must begin with a selection of solvents which cover a sufficient range of values of these two parameters. As well, it is important that the two parameters do not correlate strongly, so that effects dependent upon each can be distinguished. Table 3 lists the characteristics of a reasonable choice of solvents for study of $W(CO)_5L$ systems along with a collection of quantum yield results. The range of thermal conductivities is from 138 to 209 $W\text{ cm}^{-1}\text{ }^\circ\text{C}^{-1}$. The highest and lowest values are associated with solvents of similar viscosity. Solvent fluidity covers the range from 0.3392 to 3.1546 cp^{-1} . Here, the highest and lowest values are associated with solvents of similar thermal conductivity. There is a good opportunity to distinguish the effects associated with each parameter.

We can begin with consideration of the dependence of quantum yields for production of $W(CO)_5S$ from $W(CO)_5py$ as a function of solvent fluidity. Fig. 3 shows quantum yields plotted against fluidity for experiments using irradiation at 313 nm (■) and 458 nm (◆) [13]. These two are the extremes of the singlet region. It is clear that there is a very good correlation at 313 nm but that the 458 nm results are close to a scatter diagram. Statistical analysis shows that the correlation coefficients r^2 for the relation between quantum yield and fluidity are 0.732 and 0.931 for the wavelengths 436 nm and 365 nm respectively. A two parameter correlation including thermal conductivity merits consideration.

In order to weight the two solvent parameters comparably, it is useful to introduce

Table 3
Solvent dependence of quantum yield

Solvent	Solvent parameters ^a		Quantum yield ^b			
	θ	$1/\eta$	313 nm	365 nm	436 nm	457.9 nm
Acetone	179	3.1546		0.67(0.03) ³¹	0.68(0.02) ⁵	0.61(0.04) ¹³
Methanol	209	1.675	0.57(0.06) ²⁰	0.62(0.02) ²⁴		0.42(0.01) ¹¹
Butanol	168	0.3392	0.50(0.03) ³⁰	0.53(0.03) ²²	0.45(0.01) ¹⁰	
$CHCl_3$ -1-hexene	138	1.7240	0.59(0.03) ²⁶	0.55(0.01) ²⁴	0.52(0.01) ⁸	0.45(0.05) ⁶
Toluene-1-hexene	160	1.6949	0.57(0.03) ³²	0.58(0.01) ²¹	0.55(0.01) ⁹	0.39(0.02) ⁵
Hexane-1-hexene	142	3.0675	0.67(0.05) ⁵	0.62(0.02) ²⁵	0.62(0.02) ⁵	0.50(0.02) ⁵

^a θ ($W\text{ cm}^{-1}\text{ }^\circ\text{C}^{-1}$) is thermal conductivity taken from the International Critical Tables. $1/\eta$ (cp^{-1}) is fluidity calculated as the inverse of the viscosity η taken from the Handbook of Chemistry and Physics, CRC Press, Boca Raton, FL, 1st student edn., 1988. Solvents with 1-hexene are 24:1 solvent:1-hexene (v:v). ^b Values in parentheses are standard deviations; superscripts record the number of trials.

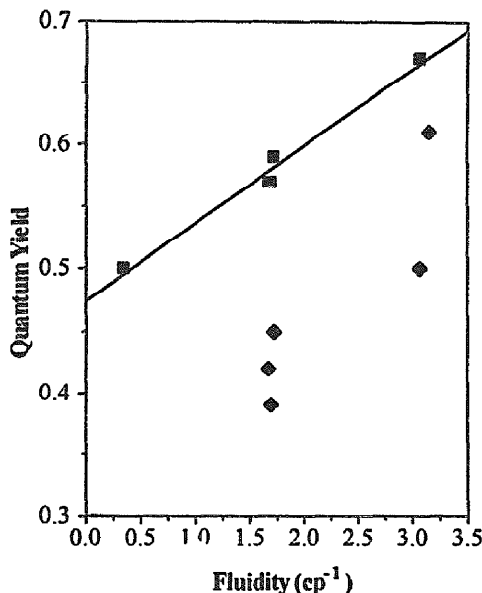


Fig. 3. Quantum yield vs. fluidity at 313 nm irradiation (■) and at 457.9 nm irradiation (♦). The equation for 313 nm data obtained from linear regression is: $\Phi = 0.121(\eta')^{-1} + 0.474$, with $r^2 = 0.9903$.

two reduced parameters. We define $\eta' = \eta/\eta_{\text{ref}}$ and $\theta' = \theta/\theta_{\text{ref}}$ where the reference value (ref) is chosen as the average value of the parameter in the set (the mean fluidity η_{ref} is 1.9425 cp^{-1} ; the mean thermal conductivity θ_{ref} is $166 \text{ W cm}^{-1} \text{ }^\circ\text{C}^{-1}$). With the reduced parameters, the different units of the two quantities do not disguise their relative roles. Eq. (1) defines a two parameter correlation where a is the coefficient for fluidity dependence, b is the coefficient for thermal conductivity dependence, and c is the intercept (which may describe reaction in a sort of 'glassy hard sphere' medium).

$$\Phi = a(1/\eta') + b\theta' + c \quad (1)$$

The values of a , b and c for irradiation at 365 nm and 436 nm are collected in Table 4 along with appropriate confidence intervals [13]; the two parameter regression of the data improves the correlation coefficients r^2 to 0.987 and 0.998 respectively.

The ratios of the coefficients a and b are 1.89 and 1.51 for 365 nm and 436 nm respectively. At both wavelengths in the lower ligand field singlet region, thermal conductivity seems to be a substantially more important parameter than fluidity. It is important to note that the conclusion that circumstances are parallel at these two wavelengths but different from circumstances at 313 and 458 nm are not dependent upon statistical analysis parameters alone. Qualitatively, a significant solvent order for quantum yields (butanol < chloroform < toluene < hexane, methanol < acetone), which is not the fluidity order seen at 313 nm, holds at both of these intermediate

Table 4
Constants in the empirical equations for ϕ at 365 and 436 nm^a

Constant	365 nm	436 nm
<i>a</i>	0.090 ± 0.020	0.146 ± 0.021
<i>b</i>	0.170 ± 0.063	0.221 ± 0.129
<i>c</i>	0.337 ± 0.063	0.205 ± 0.129

^a Constants are reported as constant $\pm 95\%$ confidence range determined from multiple regression analysis and Student's *t* distribution; *a*: coefficient of reduced fluidity; *b*: coefficient of reduced thermal conductivity; *c*: intercept.

wavelengths. The contrast between the 313 nm results and the pair, 365 and 435 nm, is clear. At 458 nm, where the ligand field triplet is irradiated with some overlap of the singlet tail, no parameter of solvent dominates, and correlations cannot be reliably established with the present range of solvent parameters and quantum yields. The quantum yields cannot be 'explained' by either fluidity or thermal conductivity factors. There is a trend in the results. At high excitation energy fluidity seems to be an adequate parameter. At intermediate energies, thermal conductivity plays a definable leading role. At low energy, the role of the two factors becomes unclear. We gain confidence in the two parameter analysis from this systematic trend. It is worth noting that quantum yields tend to be lower overall at 458 nm, as reported earlier for the limited solvent sets [4].

5. Interpretation

At 313 nm the results provide a classic mechanical cage effect correlation with fluidity, which suggests quantum yield determined by escape from the primary solvent cage. Given that room temperature cages have nanosecond lifetimes, it is perhaps not surprising that this simple behaviour is observed for processes determined in such short time scales only when there is large excess energy to drive the departing ligand. We have estimated [13] that the minimum energy required for fission of the W–py bond is less than $15\,300\text{ cm}^{-1}$. At 313 nm the excess energy is at least $16\,600\text{ cm}^{-1}$ (199 kJ mol^{-1}). From the point of view suggested by the molecular dynamics simulation, escape is possible before the energy dissipating solvent cages are well formed. If this analysis is correct, the fact that yields at this wavelength can be lower than yields at longer wavelength, an interesting fact first observed by Wrighton et al. [14], must be a consequence of the role of electronic factors. High yields at 365 nm were in fact attributed to electronic factors [14] (and the vibronic coupling in the primary excitation event) before solvent effects were fully explored and the argument remains persuasive [4].

At 365 nm the excess energy is near $12\,000\text{ cm}^{-1}$ (144 kJ mol^{-1}). It is apparent in this case that increasing thermal conductivity is favourable to product formation. If partners remain trapped for a measurable time within the solvent cage, the dominant factor probably becomes the prompt 'cooling' to the surroundings. It is

plausible that recrossing in the neighbourhood of the transition state favours return to the initial complex and ultimate relaxation to the original ground state. Similar phenomena under 436 nm irradiation suggest a similar path. However, the declining ratio of thermal conductivity coefficient to fluidity coefficient suggests that there may be a longer-lived trap state which is accessible at lower energies. In this case we might find an approach to behaviour associated with a nearly thermally equilibrated excited state. The loss of significant correlation to solvent dynamic parameters in the experiments using 458 nm irradiation supports this speculation. There is evidence that a triplet can have nanosecond life in some environments. Perhaps the triplet does approximate reaction from a thermally equilibrated excited state where the solvent insensitivity of thermal reactions of ground states of carbonyl complexes is mimicked.

The case of $\text{W}(\text{CO})_5\text{py}$ provides the level of complexity needed to reveal that the possibilities anticipated by Harris et al. [8] (see Fig. 1) can indeed be resolved in the behaviour of a polyatomic system. We see here (at least in principle, if our analysis of the system on the basis of the present data is not too grossly simplified) that we can identify the factors favouring: (1) early dissociation; (2) relaxation toward a product surface without recrossing; (3) trapping to a longer-lived excited state. This review has not covered the other major line of evidence for the assignment of this level of complexity to the pathways. There is selectivity in the formation of $\text{W}(\text{CO})_5\text{S}$ whenever *S* has the capacity to supply more than one donor atom. For example, an alcoholic solvent can be shown to have produced both alkyl group and hydroxyl group (C–H and O–H) coordination to W in a variable and non-statistical distribution at a time delay of 50 ps [7]. The selectivity has been linked to the differences in vibronic characteristics of excitation at different wavelengths, but it certainly illustrates the multiplicity of detailed pathways in these reactions.

Acknowledgements

The research from our laboratory was supported by the Natural Sciences and Engineering Research Council of Canada. We thank Dr. Elspeth Lindsay, Dr. Antonin Vicek, Jr., and Professor D.J. Stufkens for continuing stimulation. We report with great sadness that a serious stroke has deprived us of the wisdom and experimental skill of Dr. D.K. Sharma, who operated the Canadian Centre for Picosecond Spectroscopy for more than a dozen years. We wish him a speedy return to a satisfying quality of life.

References

- [1] A.G. Joly and K.A. Nelson, *Chem. Phys.*, 152 (1991) 69.
- [2] C. Moralejo, D.K. Sharma and C.H. Langford, *Inorg. Chim. Acta*, 126 (1987) 111.
- [3] J. Nasielski and A. Colas, *Inorg. Chem.*, 34 (1978) 1476.
- [4] C. Moralejo, C.H. Langford and D.K. Sharma, *Inorg. Chem.*, 28 (1989) 2205.

- [5] C. Moralejo and C.H. Langford, *Inorg. Chem.*, 30 (1991) 567.
- [6] E. Lindsay, A. Visek and C.H. Langford, *Inorg. Chem.*, 32 (1993) 3822.
- [7] C. Moralejo and C.H. Langford, *J. Photochem. Photobiol. A: Chem.*, 59 (1991) 285.
- [8] A.L. Harris, J.K. Brown and C.B. Harris, *Annu. Rev. Phys. Chem.*, 35 (1988) 341.
- [9] S. Wieland, R. van Eldik, D.R. Crane and P.C. Ford, *Inorg. Chem.*, 28 (1989) 3663.
- [10] J.T. Hynes, *Annu. Rev. Phys. Chem.*, 36 (1985) 573.
- [11] T. Elsaesser and W. Kaiser, *Annu. Rev. Phys. Chem.*, 42 (1991) 83.
- [12] P.A. Reito, E. Bindewald and D. Chandler, *Nature*, 375 (1995) 129.
- [13] C.H. Langford and L.E. Shaw, in preparation.
- [14] M. Wrighton, G.S. Hammond and H.B. Gray, *Mol. Photochem.*, 5 (1973) 179.